



DEPARTMENT OF PHYSICS

Master's degree in Advanced Methods in Particle Physics

MEASUREMENT OF MATTER-ANTIMATTER ASYMMETRIES WITH THE LHCb EXPERIMENT

Study of asymmetry in $B^\pm \rightarrow h^\pm h^+ h^-$ decay

Supervisors:

M.Sc. Luca Balzani
M.Sc. Marco Colonna
M.Sc. Luca Toscano

Lab report of:

Giulio Giamello
Cem Kurt

Summer Semester 2025

Contents

Introduction	1
1 Theoretical background	2
1.1 The Sakharov conditions	2
1.2 CP violation in the Standard Model	2
1.2.1 Cabibbo-Kobayashi-Maskawa matrix	3
1.2.2 CP violation in weak decays of B-meson	4
2 LHCb Detector	6
2.1	6
3 Experimental analysis	10
3.1 Analysis strategy	10
3.2 Data analysis	11
3.2.1 Simulated data	11
3.2.2 Real data	14
3.2.3 Global CP asymmetry	16
3.2.4 Dalitz plots	17
3.2.5 Mass ordered Dalitz plot	19
3.2.6 Local CP asymmetry	20
Conclusions	24

Introduction

The origin and evolution of our universe is an open question still nowadays. One of the most profound mysteries is the matter-antimatter asymmetry. From what we know, the Big Bang should have produced equal amounts of matter and antimatter; however, our universe is overwhelmingly composed of matter. This imbalance poses a grand challenge to our understanding of fundamental physics and the Standard Model of particle physics; as there is currently no known mechanism that can fully account for the conditions that lead to a matter-dominated universe. For this lab, we are going to study one of the possible explanations for the matter-antimatter asymmetry in the form of decay rate comparisons for matter and antimatter states.

Most of the processes that are of interest in our discipline occur within time and length scales that are practically impossible to record or observe. The strong and electroweak interactions that we are trying to understand can only be probed by the rigorous analysis of the final and initial states of the particles involved in these interactions. The strategy scientists decided to employ in order to study these fundamental interactions has evolved ever so slightly since the 50's, when CERN was founded. The main goal of the strategies being to minimize the interference from all the technical difficulties as much as possible and extract the useful science from the experimental data. Today, in Large Hadron Collider (LHC), we are colliding protons with 13 TeV center-of-mass energies at 40×10^{16} times per second. Such high energies and high rate of collisions unlock the possibility of analyzing many processes. Our purpose built detectors manage to record the aftermath or the final states of the fundamental particle interactions very well; however, the flipside of the coin, the massive data that we collect needs to be analyzed with many layers of similarly purposefully designed hardware systems, software systems and reconstruction. The detector measurement for any process in LHC is buried under every other process that happens at the same time. Since we are interested in figuring out the details of a specific process, we always need to come up with a strategy to select only the signal for the process we want to study, which is what we will be following up fully in this lab.

In more detail: the decay process of our interest in this analysis is the B-meson decay $B^+ \rightarrow K^+ K^- K^+$.

Chapter 1

Theoretical background

1.1 The Sakharov conditions

For the current state of matter-antimatter asymmetry to occur in our universe, the Russian physicist Andrei Sakharov outlines three fundamental criteria that must be satisfied[?]. First, there must be baryon number violation. This means that certain processes in the early universe must have allowed the net number of baryons (matter particles like protons and neutrons) to change. Second, C and CP symmetry must be violated, so that the laws of physics treat matter and antimatter differently; otherwise, any processes generating baryons and anti-baryons would occur at the same rate, cancelling each other out. Third, the universe must have gone through periods of thermal non-equilibrium, since in a perfectly balanced thermal state, even asymmetric processes would be reversed and no lasting imbalance would emerge. While the Standard Model includes limited CP violation and mechanisms for baryon number violation, their effects are too weak to explain the vast dominance of matter observed. For this lab, we are going to try take part in improving our understanding of this asymmetry through precision measurements of CP violation in LHCb.

1.2 CP violation in the Standard Model

In the Standard Model, the CP symmetry is the combination of C and P symmetries, where C is the *charge conjugation* and P is the *parity* (inversion of spacial coordinates) symmetry. CP violation arises from the asymmetric coupling of the weak interaction to left-handed and right-handed fermions, which is described by the charge current interactions of the W bosons. These interactions end up only coupling to specific charge combinations of quark flavours (up-type quarks \Leftrightarrow down-type quarks). Since quarks come in three generations, couplings between them via weak interactions are described by a 3×3 complex unitary matrix known as the Cabibbo-Kobayashi-Maskawa (CKM)

matrix[?].

1.2.1 Cabibbo-Kobayashi-Maskawa matrix

The CKM matrix is what accounts for the mixing of different quark flavours and introduces a complex phase that can lead to the violation of Charge-Parity symmetry. Algebraically, the CKM matrix V_{CKM} puts in relation expresses the weak eigenstate (d, s, b) with the mass eigenstate (d', s', b') thorough a rotation transformation (the matrix itself) of the two basis. It is a 3×3 matrix expressed at its simple form as :

$$\begin{pmatrix} d' \\ s' \\ b' \end{pmatrix} = \underbrace{\begin{pmatrix} V_{ud} & V_{us} & V_{ub} \\ V_{cd} & V_{cs} & V_{cb} \\ V_{td} & V_{ts} & V_{tb} \end{pmatrix}}_{V_{CKM}} \cdot \begin{pmatrix} d \\ s \\ b \end{pmatrix}$$

Each element V_{ij} represents the strength of the transition from an up-type quark "i" (u, c, t) to a down-type quark "j" (d, s, b). These elements are complex numbers, and their magnitudes determine the probabilities of various weak decays. There are 4 degrees of freedom that remain in this matrix due to it being complex-unitary, 3 mixing angles and 1 complex phase. The presence of the complex phase is what allows for CP violation where the processes involving quarks or anti-quarks can proceed with different transition probabilities if the matrix elements have non-zero imaginary parts. This complex phase arises from the 3 generational nature of the Standard Model. The matrix is analogous to a rotation matrix in 3-D space + the complex phase:

$$V_{CKM} = \begin{pmatrix} c_{12}c_{13} & s_{12}c_{13} & s_{13}e^{-i\delta_{13}} \\ -s_{12}c_{23} - c_{12}s_{23}s_{13}e^{i\delta_{13}} & c_{12}c_{23} - s_{12}s_{23}s_{13}e^{i\delta_{13}} & s_{23}c_{13} \\ s_{12}s_{23} - c_{12}c_{23}s_{13}e^{i\delta_{13}} & -c_{12}s_{23} - s_{12}c_{23}s_{13}e^{i\delta_{13}} & c_{23}c_{13} \end{pmatrix}$$

Where the terms are the sine (s) or cosine (c) combinations ($c_{ij} \equiv \cos \theta_{ij}$) of the three mixing angles ($\theta_{12}, \theta_{13}, \theta_{23}$) and one CP violating phase (δ).

If we complement this theory with experimental results and formulate it as such that V_{CKM} would be a unity matrix if there were no quark mixing, we get the Wolfenstein parametrization expression (Approximation using $\lambda \approx 0.224$ at third order with parameters A, ρ, η):

$$V_{CKM} = \begin{pmatrix} 1 - \frac{\lambda^2}{2} & \lambda & A\lambda^3(\rho - i\eta) \\ -\lambda & 1 - \frac{\lambda^2}{2} & A\lambda^2 \\ A\lambda^3(1 - \rho - i\eta) & -A\lambda^2 & 1 \end{pmatrix} + O(\lambda^4)$$

Where the terms are:

$$\lambda \equiv |V_{us}| \equiv s_{12} \approx 0.224 \quad \text{and} \quad A \equiv \frac{s_{23}}{s_{12}^2} \approx 0.82$$

with the CP violating (complex phase) terms being present only in V_{ub} and V_{td} couplings at λ^3 order:

$$\rho = \text{Re} \left(\frac{s_{13} e^{-i\delta}}{s_{12} s_{23}} \right) \quad \text{and} \quad \eta = -\text{Im} \left(\frac{s_{13} e^{-i\delta}}{s_{12} s_{23}} \right)$$

This theoretical result tells us that for studying the involved CP-violation, we should analyse a weak process involving top-down or bottom-up quark transition.

1.2.2 CP violation in weak decays of B-meson

The B-meson decay processes in this analysis are of interest because their branching ratio is dependent upon the coupling elements from the V_{CKM} that include the possibly CP violating phase term: V_{ub}^* (and V_{ub} for B^- respectively) highlighted in [Figure 1.1](#):

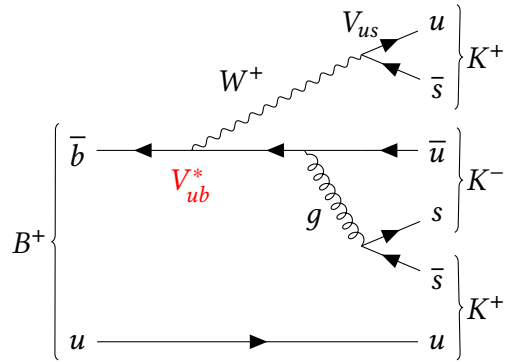


Figure 1.1: (one possible) Feynman Diagram for the process: $B^+ \rightarrow K^+ K^- K^+$.

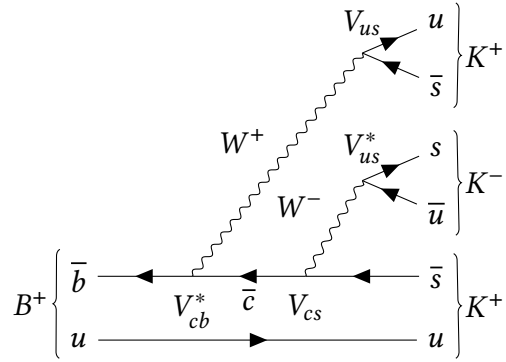


Figure 1.2: (another) Feynman Diagram for the process: $B^+ \rightarrow K^+ K^- K^+$.

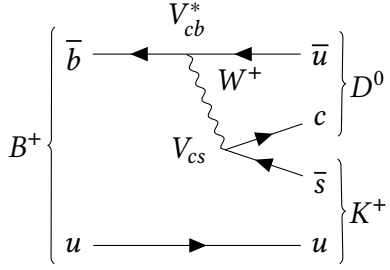


Figure 1.3: Feynman Diagram for the resonant process: $B^+ \rightarrow D^0 K^+ \rightarrow K^+ K^- K^+$.

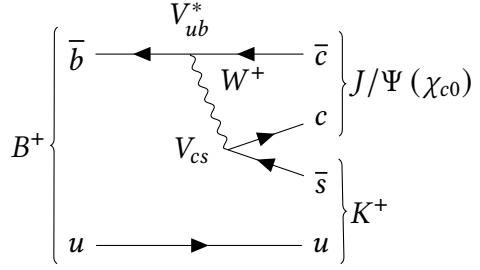


Figure 1.4: Feynman Diagram for the resonant process: $B^+ \rightarrow J/\Psi(\chi_{c0}) K^+ \rightarrow K^+ K^- K^+$.

The final counts between B^+ and B^- decay processes should only differ via the possibly differing strengths of the coupling V_{ub}^* , shown in red. The quantity we define and measure will called the CP asymmetry “ A_{CP} ”:

$$A_{CP} = \frac{N^+ - N^-}{N^+ + N^-}$$

Where N^- is the amount of recorded $B^- \rightarrow K^- K^+ K^-$ events and N^+ is the amount of recorded $B^+ \rightarrow K^+ K^- K^+$ events.

Chapter 2

LHCb Detector

2.1

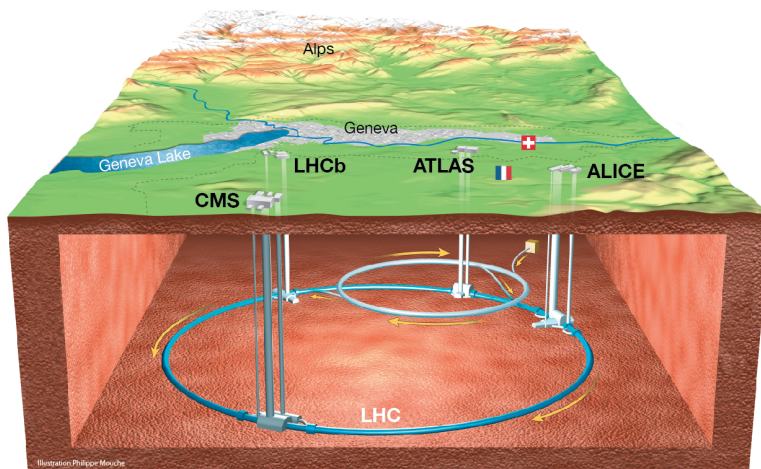


Figure 2.1: LHC schema with ALICE, Atlas, CMS and LHCb at CERN.

The LHCb detector is part of one of the four large experiments set up on different points of the circular accelerator design of LHC, at CERN. The detectors are constructed around collision points where the accelerated beams of protons are crossed with each other 40×10^{16} times per second. Unlike rest of the detectors at LHC, the LHCb detector is built to detect particles from a singular direction, with the official name for the design being, "Single arm forward spectrometer". It can detect particles coming from the interaction point in the pseudorapidity range between $2 < \eta < 5$ and it is designed

philosophy is geared towards measuring b (bottom) and c (charm) hadron properties alongside CP violation. [?]

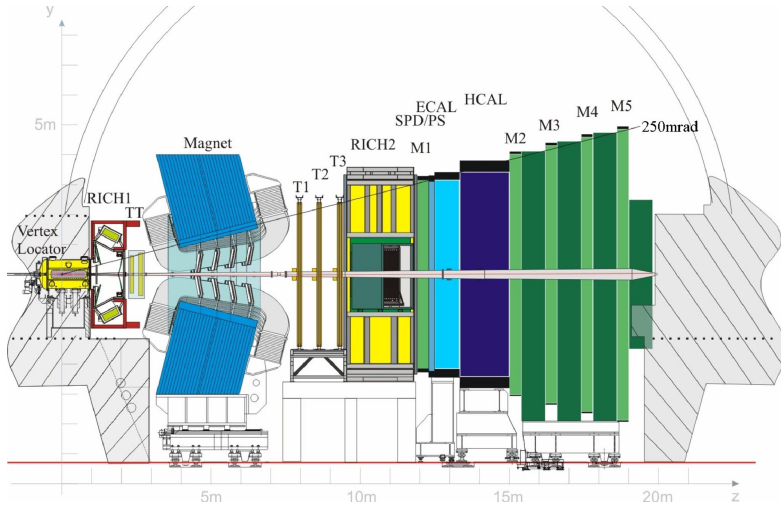


Figure 2.2: The LHCb detector. Detector elements from left to right: I-Vertex locator, II-RICH1, III-Trigger tracker(TT), IV-Dipole magnet, V-Outer trackers(T1,T2 and T3), VI-RICH2, VII-Muon detector 1, VIII-Hadronic and electromagnetic calorimeters, IX-Muon detector 2,3,4 and 5.

The LHCb detector is made up of the following components:

1. VELO (Vertex locator)

Purpose: Precise reconstruction of primary and secondary vertices coming from the collision.

Features: Silicon-strip detectors close to the beam line, retractable during the beam injection phase.

2. TT Station (Trigger tracker)

Purpose: Tracking particles before entering the magnetic field.

Features: Silicon microstrip detector upstream of the magnet.

3. Dipole magnet

Purpose: Bends charged particles, making it possible to measure their momentum later.

Features: Approximately 4 T·m integrated magnetic field special to the forward spectrometer design.

4. Tracking stations (T1,T2 and T3)

Purpose: Tracking particles after leaving the magnetic field (tracking charged particles for momentum measurement).

Features: Straw tube drift chambers that cover a large radius.

5. RICH detectors (Ring-imaging Cherenkov detectors)

Purpose: Particle identification (separating pions, kaons, protons).

Features: Based on the Cherenkov effect, can measure the velocity of the passing particles by recording the angle of which their Cherenkov radiation is received. The equation for the angle in terms of the velocity of the radiating particle is:

$$\cos(\theta_C) = \frac{1}{n \cdot \frac{v}{c}} = \frac{c}{nv}$$

where the n is the refractive index of the detector material.

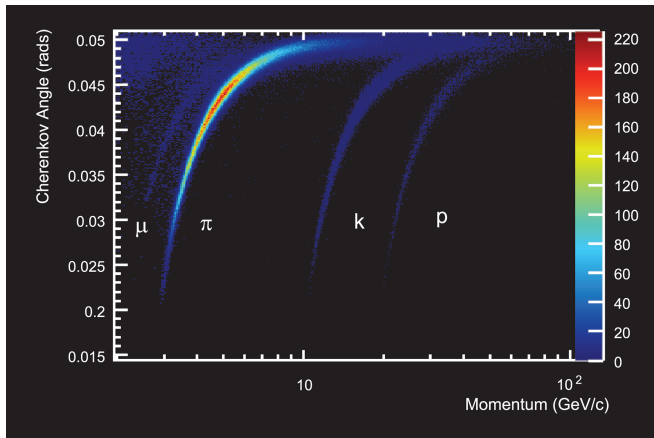


Figure 2.3: Possible particles and their momentum via a given Cherenkov angle.

6. Calorimeters

Purpose: Measuring the energy of electrons, photons, and hadrons via particle shower.

Features:

- **Scintillating Pad Detector:** Electron/photon identification.
- **Preshower Detector:** Distinguishes electrons from hadrons.
- **Electromagnetic Calorimeter:** Measures energy of electrons and photons.

- **Hadronic Calorimeter:** Measures energy of hadrons (neutral hadrons like neutrons are primarily stopped here).

7. Muon system

Purpose: Muon identification.

Features: Five stations (M1–M5) using Multi-wire proportional chambers and gas-electron multipliers. The M1 station is before the calorimeters and M2 to M5 after, with shielding in between.

Chapter 3

Experimental analysis

3.1 Analysis strategy

The goal is to understand and measure the differences in the behaviour of matter and antimatter with data recorded by the Run 1 of the LHCb experiment.

For this purpose, the analysis performed here compares the rates for the decays $B^+ \rightarrow h^+h^+h^-$ and its antiparticle equivalent $B^- \rightarrow h^-h^-h^+$, where h^\pm is a pion π^\pm or a kaon K^\pm . The B^+ meson is composed of a \bar{b} quark and u quark. The pion π^+ is composed of a \bar{d} and u quarks, the kaon K^+ of a \bar{s} and u quarks. The decays studied proceed through the weak force (via W^\pm bosons), where the CP symmetry is known to be violated¹.

Therefore we studied *global* and *local* CP violation, comparing the number of B^+ meson with the number of its anti-particle B^- . Since the value of CP violation might vary in different kinematic regions, then we focused on *local* CP violation, meaning only on those regions were it is maximally violated.

In this analysis, we focus in particular the decays $B^\pm \rightarrow K^\pm K^+K^-$.

Practically, the following programmes and frameworks are used to perform the analysis: [Python](#), [Jupyter](#), [Root](#) [?].

The data we have at our disposal are in the file format common to LHC experiments, with the extension `.root`. Often files of this type are called [tuple](#). In this project, there are three different tuples:

- `PhaseSpaceSimulation.root`, contains simulated data for the decay $B^\pm \rightarrow K^\pm K^+K^-$;
- `B2HHH_MagnetUp.root`, contains data recorded by the LHCb experiment in 2011 reconstructed with a decay $B^\pm \rightarrow h^\pm h^+h^-$ with “up” magnet polarity;

¹The observation of CP violation requires interference between two decay routes to the same final state.

- `B2HHH_MagnetDown.root`, contains data recorded by the LHCb experiment in 2011 reconstructed with a decay $B^\pm \rightarrow h^\pm h^+ h^-$ with “down” magnet polarity.

We handle the three `.root` dataset file in Python converting those in the format of a `pandas.DataFrame` with the help of the Python package: [root-pandas](#).

3.2 Data analysis

3.2.1 Simulated data

We import the simulated data `.root` file as a `pandas.DataFrame`:

```
1 sim_data = read_root('/data/PhaseSpaceSimulation.root')
```

The data contains information about “events” that were observed in the detector. An event refers to the particles produced when two proton bunches of the beams collided at the LHC.

The detector has been used to reconstruct tracks that may have come from the kaons; in the `pandas.DataFrame` we have access to the measured momenta ([Figure 3.1](#)), charge, and likelihood of the tracks being kaons.

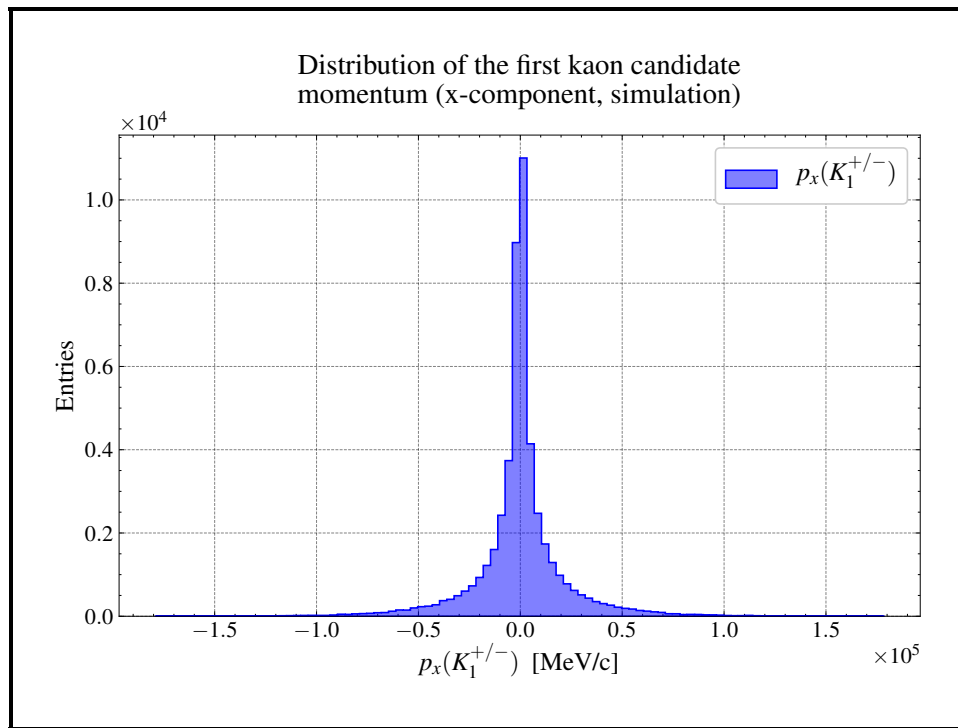


Figure 3.1

From the momentum for each axis of the three children particles we can compute the *magnitude* of this quantity,

$$(3.1) \quad \left\| \underline{p}(K^i) \right\| = \sqrt{p_x^2(K^i) + p_y^2(K^i) + p_z^2(K^i)}$$

where $i \in \{1, 2, 3\}$.

that has the following distribution ([Figure 3.2](#)),

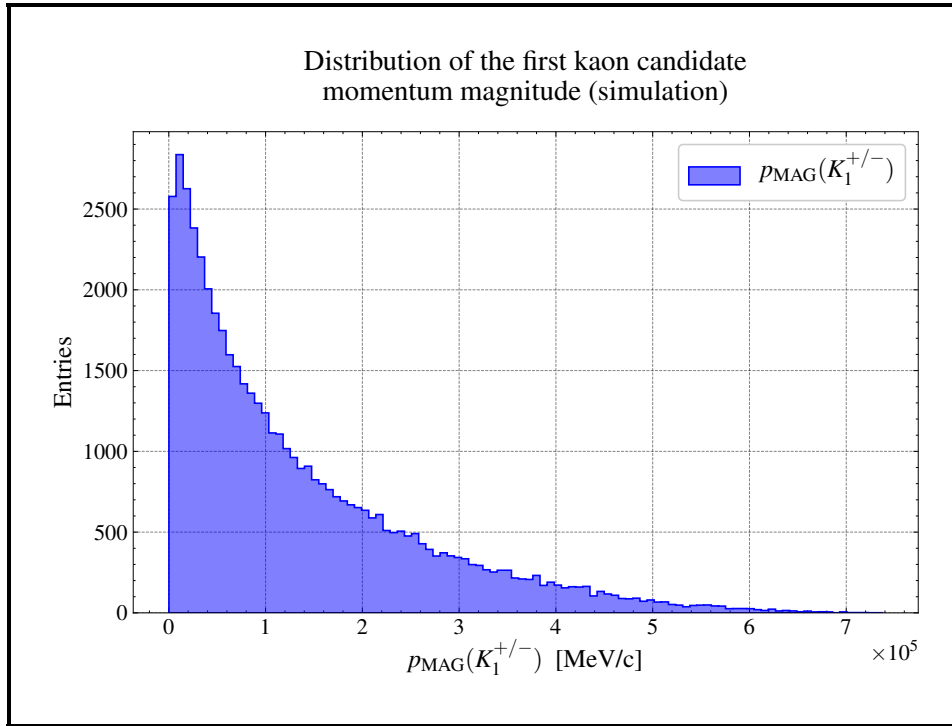


Figure 3.2

The knowledge of the momentum magnitude with the kaon K^\pm mass from the [PDG](#) [?] allow us to compute the energy of the children particles from the *energy-momentum relation*: $E^2 = p^2 + m^2$,

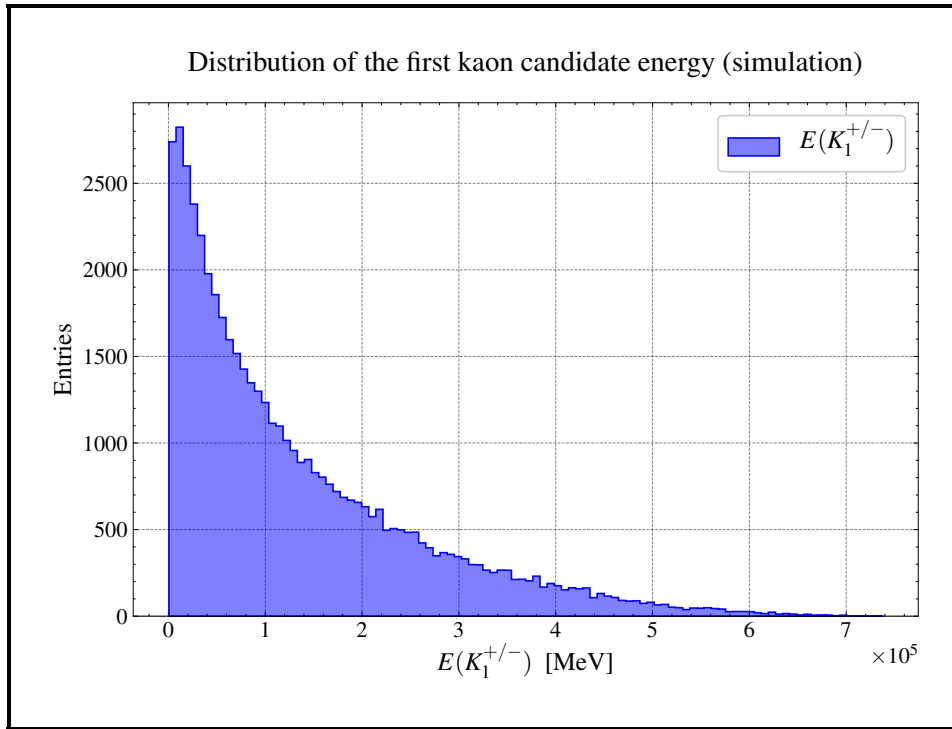


Figure 3.3

Once computed the energy of the three kaons, taking advantage of the *conservation of energy and momentum*, we can compute the energy and momentum of the mother particle B^\pm as:

$$(3.2) \quad E(B) = \sum_{i=1}^3 E(K^i)$$

and

$$(3.3) \quad \begin{cases} p_x(B) = \sum_{i=1}^3 p_x(K^i) \\ p_y(B) = \sum_{i=1}^3 p_y(K^i) \quad \Rightarrow \quad \sqrt{p_x^2(B) + p_y^2(B) + p_z^2(B)} = \|\underline{p}(B)\| \\ p_z(B) = \sum_{i=1}^3 p_z(K^i) \end{cases}$$

finally the B^\pm invariant mass, resulting in the distribution of [Figure 3.4](#)

$$(3.4) \quad m(B) = \sqrt{E^2(B) - p^2(B)}$$

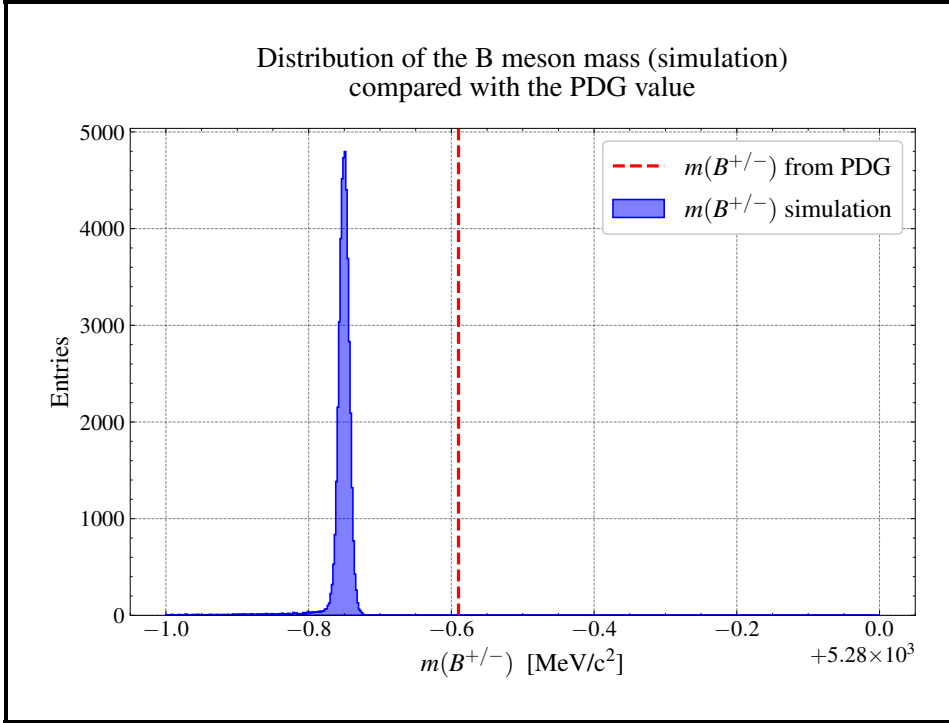


Figure 3.4

3.2.2 Real data

The *real data* have been pre-filtered to identify only events that are likely to come from B^\pm mesons, decaying into three final state charged particles (μ, π^\pm, K^\pm). We are interested only in the kaons final state, so we need to define a preselection over all the possible children particles: in order to reduce the combinatorial background and the contribution of misidentified final state particles, the probability that the particles are pions (ProbPi) and the probability that the particle is a kaon (ProbK) have been determined for each of the three candidates. In [Figure 3.5](#) and [Figure 3.6](#) are shown the probability distributions of h^1 .

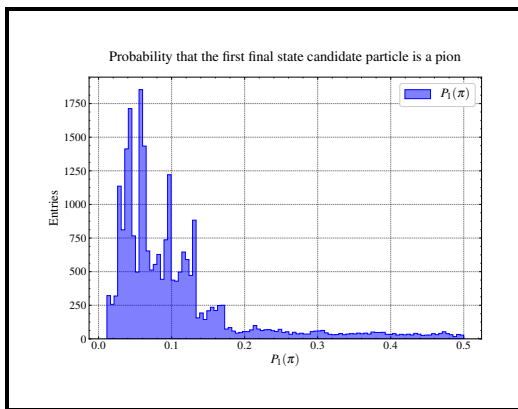


Figure 3.5

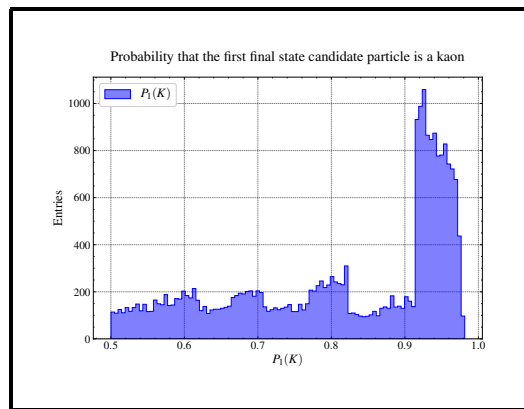


Figure 3.6

The preselection is, concretely, done using the following cuts on the real data:

Preselection			
Variable	h^1	h^2	h^3
isMuon	not	not	not
ProbPi	< 0.5	< 0.5	< 0.5
ProbK	> 0.5	> 0.5	> 0.5

Here, the preselection variable and the real data import from the Python code,

```

1 preselection = ('!H1_isMuon & H1_ProbPi<0.5 & H1_ProbK>0.5 & '+
2     '!H2_isMuon & H2_ProbPi<0.5 & H2_ProbK>0.5 & '+
3     '!H3_isMuon & H3_ProbPi<0.5 & H3_ProbK>0.5')
4
5 real_data = read_root(['/data/B2HHH_MagnetUp.root',
6                         '/data/B2HHH_MagnetDown.root'],
7                         where=preselection)

```

Once selected the “best” data for our purpose, we repeat the same procedure as in [Section 3.2.1](#) to compute the B^\pm invariant mass distribution for the real data ([Figure 3.7](#)).

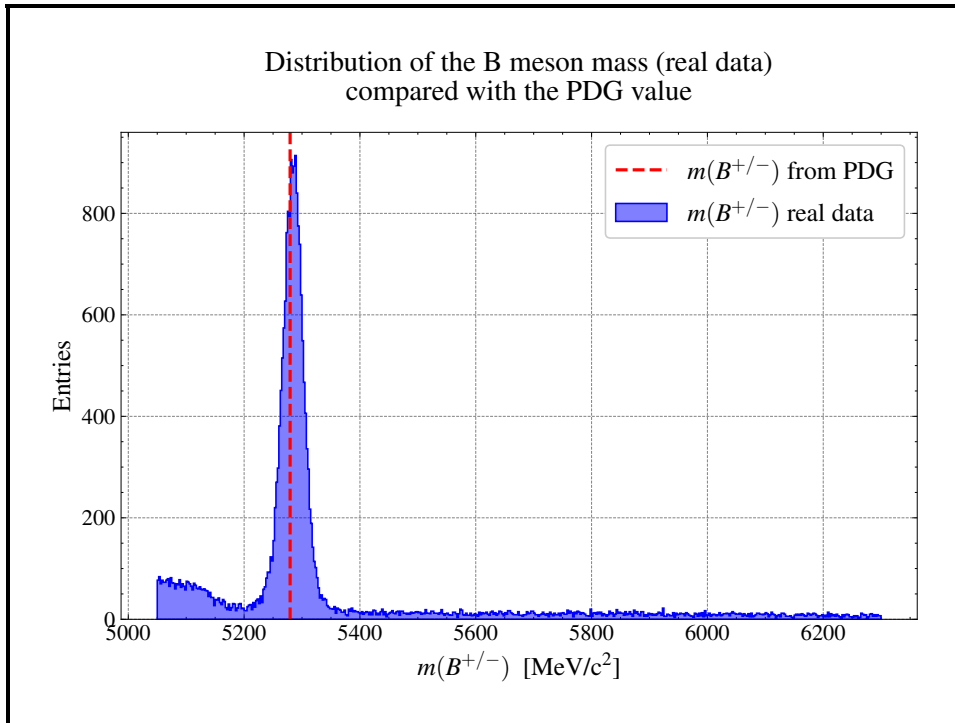


Figure 3.7

3.2.3 Global CP asymmetry

In order to quantify the *global* matter anti-matter asymmetry in this process, we compare the number of B^+ meson with the number of its anti-particle B^- . Computationally, we count the number $N^+ = 12390$ and $N^- = 11505$ of events with charge +1 and -1, respectively, in the real dataset².

This allow us to calculate the asymmetry A_{CP} and the related uncertainty σ_A and significance S_A :

²This measurement can be made more sophisticated and precise: note that in the mass distribution of B mesons there is a peak, called *signal*, and a bottom, called *background*. Therefore, it is possible to refine the selection of events by selecting only the signal, by fitting of the mass distribution to estimate the yield of signal and background events.

$$(3.5) \quad A_{\text{CP}} = \frac{N^+ - N^-}{N^+ + N^-}$$

$$(3.6) \quad \sigma_{\text{CP}}^A = \sqrt{\frac{1 - A_{\text{CP}}^2}{N^+ + N^-}}$$

$$(3.7) \quad S_{\text{CP}}^A = \frac{A_{\text{CP}}}{\sigma_{\text{CP}}^A}$$

In particle physics, a value is only considered an observation, if it is at least five standard deviations, ($> 5\sigma$). While, if it exceeds three sigma ($> 3\sigma$), it is considered evidence.

The asymmetry is corrected by the underlying production asymmetry $A_{\text{CP,prod}}$, arising from the fact that the particles are produced by proton-proton collisions. The production asymmetry is approximated with $\approx 1\%$. The final asymmetry then is calculated by:

$$(3.8) \quad A_{\text{CP,global}} = A_{\text{CP}} - A_{\text{prod}} = 0.0270$$

and through the *propagation of uncertainty*,

$$(3.9) \quad \sigma_{\text{CP,global}}^A = \sqrt{(\sigma_{\text{CP}}^A)^2 + (\sigma_{\text{prod}}^A)^2} = 0.0092$$

which gives the significance:

$$(3.10) \quad S_{\text{CP,global}}^A = \frac{A_{\text{CP,global}}}{\sigma_{\text{CP,global}}^A} = 2.9348$$

3.2.4 Dalitz plots

The decay $B^\pm \rightarrow h^\pm h^+ h^-$ can occur in two distinct ways:

- directly through three-body final state;
- via an intermediate particle, a *resonance*, through two-body decay.

For example, $B^+ \rightarrow h^+ h^+ h^-$ can proceed through the decay $B^+ \rightarrow h^+ R_0$, where R_0 is a neutral meson resonance which can decay as $R_0 \rightarrow K^+ K^-$.

An useful tool to identify resonances in the decay is the *Dalitz plot*: a bidimensional plot in the phase space that represents the possible manners in which the products of certain three-body decays can be produced. The axes of the plot are the squares of the invariant masses of two pairs of the decay products.

Notice that the kinematics of a three-body decay can be fully described using only these two variables (invariant masses of pairs of decay products), since energies and momenta of the three kaons are not independent of each other as they all come from the decay of a B meson and energy and momentum are conserved.

The simulated data do not include resonances and are therefore uniformly distributed, as can be seen in [Figure 3.8](#) and [Figure 3.9](#).

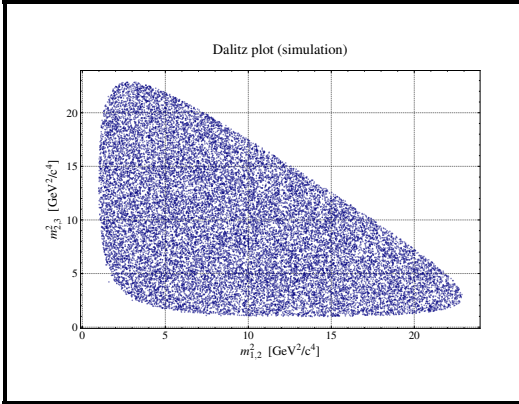


Figure 3.8: Scatter Dalitz plot of the simulated data.

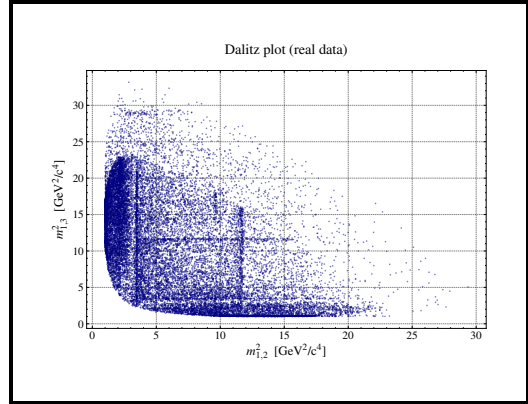


Figure 3.10: Scatter Dalitz plot of the real data.

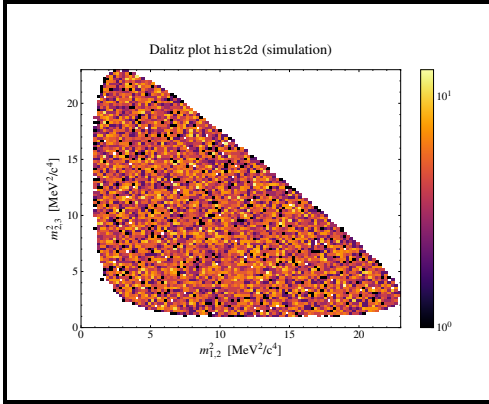


Figure 3.9: Binned Dalitz plot of the simulated data.

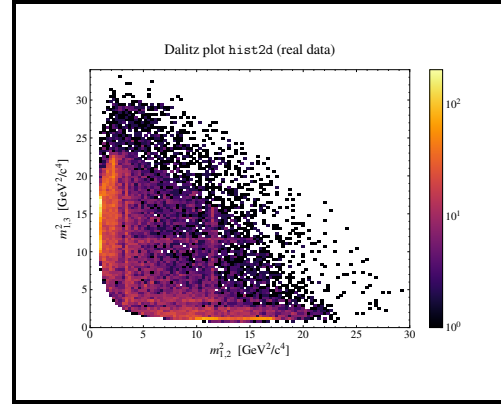


Figure 3.11: Binned Dalitz plot of the real data.

While in the real data, since two kaons always have the same charge, there are two possible resonance combinations. It is important to first look up which kaon candidates are oppositely charged: in our data the second and third kaon candidates have the same charge. Therefore the only possible combinations are $R_{1,2}^0$ and $R_{1,3}^0$. The $R_{2,3}^0$ combination would result in a charged resonance (with charge: +2 or -2), which is not provided for in the Standard Model.

So, choosing the invariant masses of $R_{1,2}^0$ and $R_{1,3}^0$ resonances as axes of the Dalitz plot, we are able to identify resonances band structures, visible in [Figure 3.10](#) and [Figure 3.11](#).

3.2.5 Mass ordered Dalitz plot

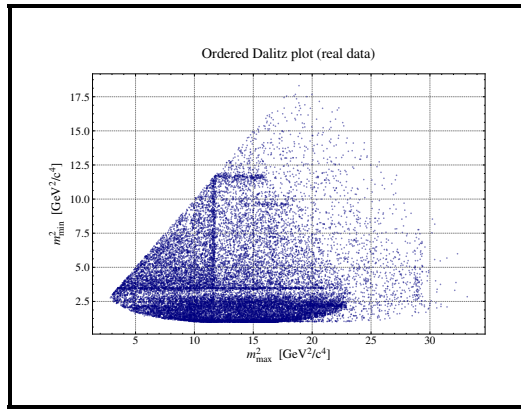


Figure 3.12

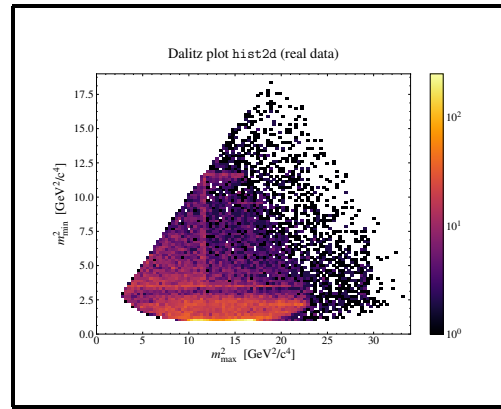


Figure 3.14

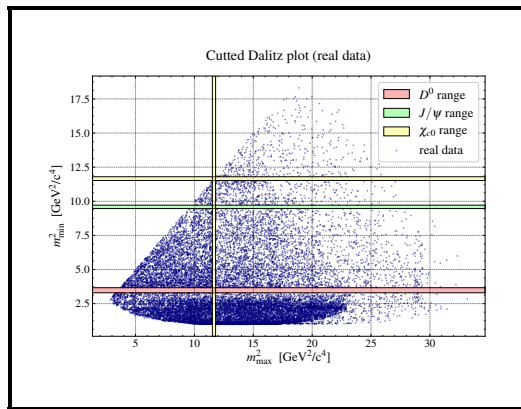


Figure 3.13

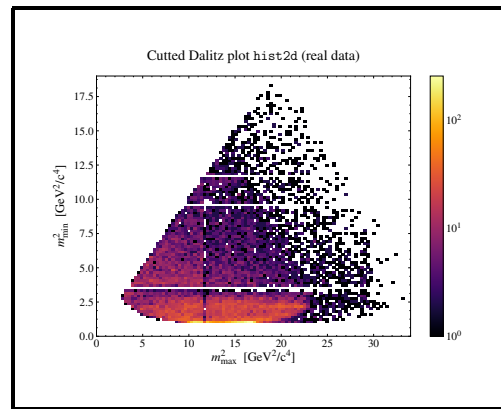


Figure 3.15

To improve the visibility of the resonances in the Dalitz plot it is useful to impose an

ordering, so we sort the two resonances in a combination of kaons with the respectively higher mass R_{\max^0} and one with the corresponding lower mass R_{\min^0} .

We now use the mass of these ordered resonances as Dalitz plot variables, thus effectively “folding” the Dalitz plot, so that one axis always has a higher value than the other. The total energy range is indeed reduced, while still remaining with the same statistics. This leads to a higher event density and therefore much “clearer” structures in the Dalitz plots.

The knowledge of resonances is of fundamental importance because it allows us to exclude from the analysis of the different possible ways in which the three-body decay can occur, those in which we are not interested: in particular, we are studying “charmless” decays and so we must remove all those resonances in which charm quarks are contained.

We can identify three of this resonances (from the PDG [?]):

- $m(D^0) = 1864.84 \pm 0.05 \text{ [MeV/c}^2]$
- $m(J/\Psi) = 3096.900 \pm 0.006 \text{ [MeV/c}^2]$
- $m(\chi_{c0}) = 3414.71 \pm 0.30 \text{ [MeV/c}^2]$

that we remove, using the following cut:

```
1 D^0 range: [ 3.3 - 3.7] [GeV^2/c^4]
2 JPSI range: [ 9.5 - 9.7] [GeV^2/c^4]
3 CHIc0 range: [11.5 - 11.8] [GeV^2/c^4]
```

This result in the Dalitz plot without resonances as in [Figure 3.13](#) and [Figure 3.15](#).

3.2.6 Local CP asymmetry

Previously, ([Section 3.2.3](#)), we calculated the global CP asymmetry, but the asymmetry value obtained was not that much significant ($< 3\sigma$). To improve this result and obtain a higher significance value, we try to calculate the *local* CP asymmetry. Indeed CP violation arises from interference between different decay chains with different intermediate resonances to a common final state. Therefore, the strength and the sign of the CP violation might vary in different kinematic regions.

For this reason, we are interested in identify those kinematic regions where CP asymmetry is maximized. Therefore, we produce two separate Dalitz plot each for B^+ and B^- decays and we look for asymmetries between those plots, as a signature of CP violation. Basically, we use `hist2d` plots to split the events in different bins and count the amount of events for each bin: in order that the statistical error on the asymmetry in each bin is not overly large, the bins need to contain a reasonable number of entries. We use a bin area of $4.6143 \text{ [GeV}^2/\text{c}^4]$.

In [Figure 3.16](#) and [Figure 3.18](#) there are the Dalitz and hist2d plots for the B^+ , while in [Figure 3.17](#) and [Figure 3.19](#) for the B^- .

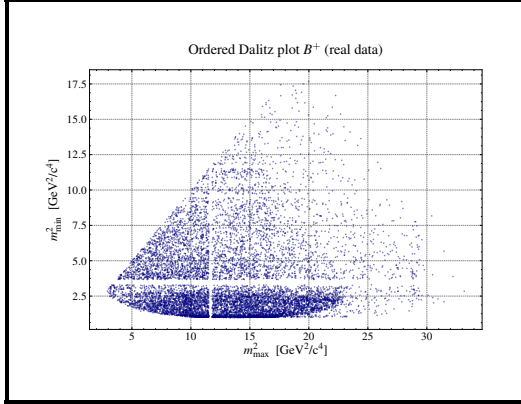


Figure 3.16

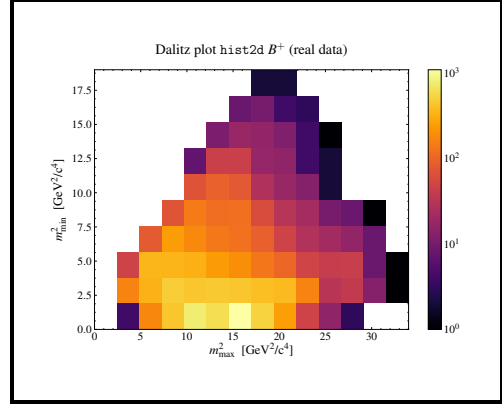


Figure 3.18

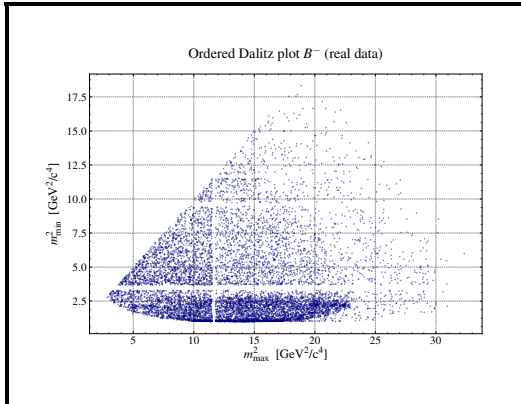


Figure 3.17

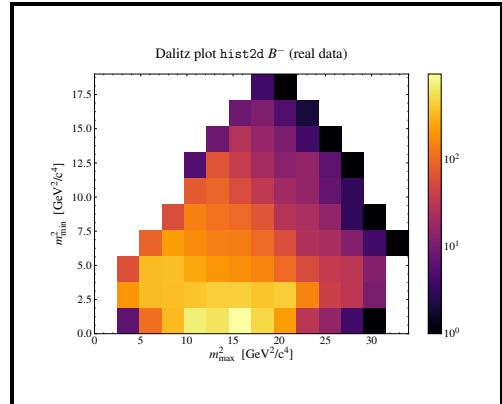


Figure 3.19

Since we used the same binning for both hist2d plots, we can calculate the CP asymmetry, A_{CP} , for each bin, comparing the number of events per bin of B^+ and B^- , and applying [Equation 3.5](#). The result is shown in [Figure 3.20](#). We have to pay attention and remember that observing a large asymmetry in some kinematic regions of the plot does not necessarily mean we have CP violation: if there are only very few events in that region of the plot the uncertainty on that large asymmetry may be large, too. Hence, the value may still be compatible with zero.

Therefore, we need to compute the uncertainty σ_{CP}^A and the significance S_{CP}^A *per bin*, as we have already done in [Section 3.2.3](#) with [Equation 3.7](#) and [Equation 3.7](#).

This procedure allow us to identify the bins with highest significance (the three marked in red in [Figure 3.21](#)), with the following values of significance:

```

1 s.T[0,2] = 3.9444
2 s.T[0,3] = 4.1711
3 s.T[1,3] = 4.7866

```

The total number of (positive and negative charged) events in this selected kinematic range is $N^+ = 1066$ and $N^- = 756$.

So we can compute the local CP asymmetry, $A_{\text{CP,local}}$, in this range and consequently the local uncertainty $\sigma_{\text{CP,local}}^A$ and the local significance $S_{\text{CP,local}}^A$.

(The computed values are corrected by the production asymmetry A_{prod} , as in [Section 3.2.3](#)).

$$(3.11) \quad A_{\text{CP,local}} = A_{\text{CP}} - A_{\text{prod}} = 0.1601$$

$$(3.12) \quad \sigma_{\text{CP,local}}^A = \sqrt{(\sigma_{\text{CP}}^A)^2 + (\sigma_{\text{prod}}^A)^2} = 0.0329$$

$$(3.13) \quad S_{\text{CP,local}}^A = \frac{A_{\text{CP,local}}}{\sigma_{\text{CP,local}}^A} = 4.8663$$

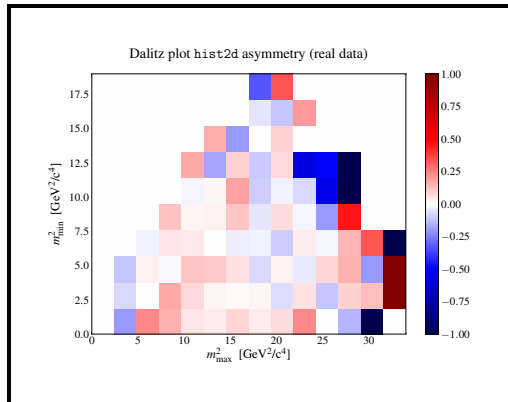


Figure 3.20

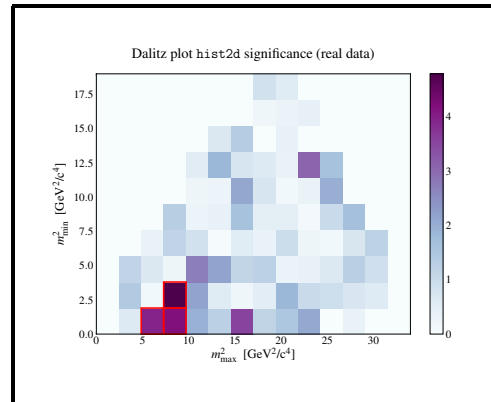


Figure 3.21

Finally, we select the B^+ and B^- real data in the maximal CP violation kinematic range and plot the mass distributions, showing the asymmetry visible in the peak, as in [Figure 3.22](#):

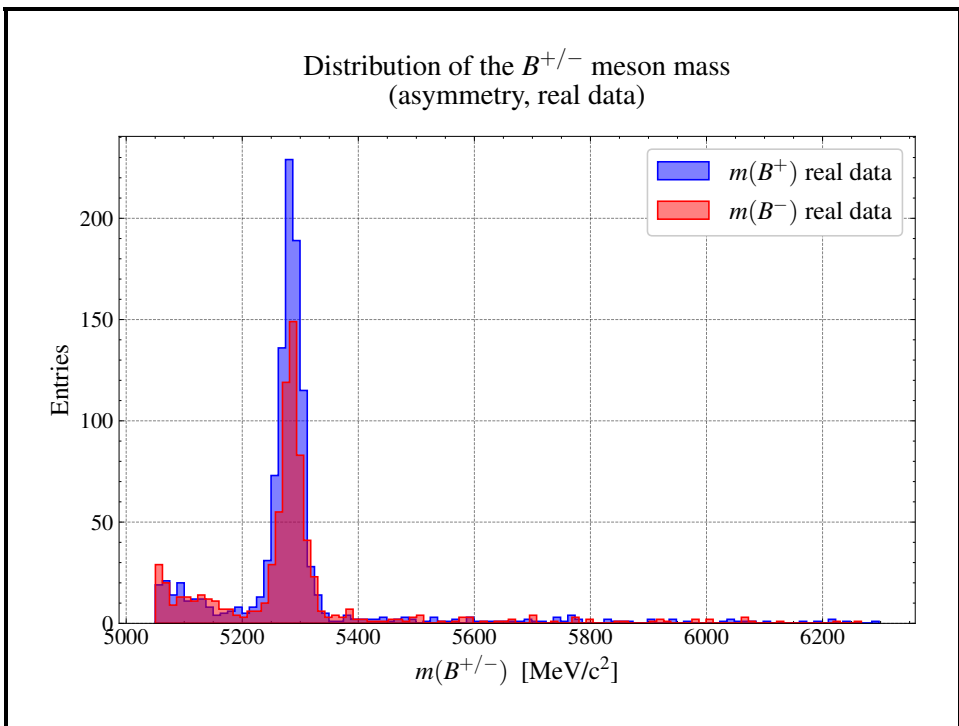


Figure 3.22

The found local CP asymmetry can therefore be called an “evidence” of a local CP asymmetry in $B^\pm \rightarrow h^\pm h^+ h^-$.

Conclusions

The aim of this experiment was to search for evidence of CP violation in the decay of charged B^\pm meson into three kaons K^\pm . the research was conducted using simulated and real dataset from the LHCb detector from 2011.

Through the use of Dalitz plots background events (decays through a charmed resonance) in the real data have been individuate and eliminate, leading to the identification of the kinematic regions where particles and antiparticles behaved in a distinctively different way. The CP asymmetry was calculated both globally and locally over these kinematic regions.

Although the significances of these results might make them out to be observations or discoveries, if we to consider other sources of uncertainties (e.g. the *production asymmetry*), we obtain only evidence.

Concluding, a more precise analysis could be conducted by taking into account such uncertainties: in fact, we could calculate the contribution of background events to the signal peak using mass sidebands or by fitting the mass distributions, in order to obtain a more precise estimation of the yield of signal and background events.